The Astrophysical Journal, 616:730–737, 2004 December 1

CHANDRA OBSERVATIONS OF THE QUIESCENT NUCLEAR BLACK HOLE OF NGC 821: EVIDENCE OF NUCLEAR ACTIVITY?

G. Fabbiano,[1] A. Baldi,[1] S. Pellegrini,[2] A. Siemiginowska,[1] M. Elvis,[1] A. Zezas,[1] and J. McDowell[1]
Received 2004 May 18; accepted 2004 July 25

ABSTRACT

We report the results of the *Chandra* ACIS-S observations of the elliptical galaxy NGC 821, which harbors a supermassive nuclear black hole ($3.5\times10^7\ M_\odot$) but does not show signs of active galactic nucleus activity. A small, 8″.5 long ($\sim$1 kpc at the galaxy's distance of 23 Mpc), possibly S-shaped, jetlike feature centered on the nucleus is detected in the 38 ks ACIS-S integrated exposure of this region. The luminosity of this feature is $L_X \sim 2.6\times10^{39}$ ergs s^{-1} (0.3–10 keV), and its spectrum is hard (described by a power law of $\Gamma = 1.8^{+0.7}_{-0.6}$ or by thermal emission with $kT > 2$ keV). We discuss two possibilities for the origin of this feature: (1) a low-luminosity X-ray jet, or (2) a hot shocked gas. In either case, it is a clear indication of nuclear activity, detectable only in the X-ray band. Steady spherical accretion of the mass losses from the central stellar cusp within the accretion radius, when coupled with a high radiative efficiency, already provides a power source exceeding the observed radiative losses from the nuclear region. A third possibility, that this feature may arise from a fortuitous distribution of luminous X-ray binaries in NGC 821, is also discussed.

Subject headings: black hole physics — galaxies: individual (NGC 821) — galaxies: nuclei — X-rays: galaxies

1. INTRODUCTION

Luminous quasars, radio galaxies, and Seyfert galaxies have long been associated with accretion onto a massive black hole (see review, Rees 1984), and the lack of nuclear emission in most galaxies has been debated alternatively as evidence for the lack of such a nuclear black hole or of fuel reaching the hole (Phinney 1983).

We now know that virtually all galaxies host supermassive black holes (SMBHs) in their nuclei. High-resolution observations of the nuclei of elliptical galaxies and bulges have established the presence of these SMBHs (Richstone et al. 1998; Magorrian et al. 1998; van der Marel 1999), whose mass is loosely correlated with the galaxy/bulge luminosity (Magorrian et al. 1998) and tightly correlated with the central velocity dispersion (Ferrarese & Merritt 2000; Gebhardt et al. 2000) and the central light concentration (Graham et al. 2001). These results remove the black hole variable from the equation and make the absence of luminous active galactic nuclei (AGNs) in these galaxies more puzzling. Although a few faint AGNs have been detected in X-rays (e.g., in the $L_X/L_E \sim 10^{-6}$–10^{-7} range, where L_E is the Eddington luminosity of the SMBH; Fabbiano & Juda 1997; Pellegrini et al. 2003a; Ho et al. 2001; Fabbiano et al. 2003), we still do not have a clear picture of what impedes the formation of a luminous AGN and how this is related to the existence and physics of a circumnuclear accretion disk (e.g., Martini et al. 2001). Given that elliptical galaxies tend to host large quantities of centrally concentrated hot interstellar medium (ISM; see Fabbiano 1989 for an early review), lack of fuel does not seem to be an option.

For example, the circumnuclear regions studied so far with the *Chandra* ACIS show the presence of hot gas close to the accretion radius; this implies, when applying the spherical Bondi accretion theory, accretion luminosity values comparable to those of luminous AGNs, if the gas close to the SMBH joins an accretion disk with a standard radiative efficiency of $\sim$0.1 (e.g., Loewenstein et al. 2001; Fabbiano et al. 2003). Since these luminosities are not observed, the options left are that the radiative efficiency is orders of magnitude lower, as in an advection-dominated accretion flow (ADAF) and its variants (e.g., Narayan 2002), or that accretion is unsteady (Binney & Tabor 1995; Ciotti & Ostriker 2001). In addition, nuclear jets can carry away a large fraction of the estimated accretion power, a possibility that has been found very reasonable for M87 (Di Matteo et al. 2003), IC 4296 (Pellegrini et al. 2003b), and IC 1459 (Fabbiano et al. 2003). NGC 821 represents another promising case to test the hypotheses above.

NGC 821 is an E6 galaxy with possible disky isophotes and centrally peaked (power-law) surface brightness (Ravindranath et al. 2001). At a distance of 23 Mpc (e.g., de Zeeuw et al. 2002), the ACIS resolution at the aim point corresponds to 55 pc. Prior to our *Chandra* observations, NGC 821 had been observed, but not detected, in X-rays with *ROSAT* ($<5\times10^{40}$ ergs s^{-1}; Beuing et al. 1999). This limit is $\sim10^5$ times below the Eddington luminosity of the nucleus, based on the SMBH mass of 2.8–$5.8\times10^7\ M_\odot$, which was measured from *Hubble Space Telescope* (*HST*) Space Telescope Imaging Spectrograph (STIS) spectra of the nuclear region coupled with dynamical modeling (Gebhardt et al. 2003). NGC 821 was observed with *Chandra* as part of a minisample of extremely faint SMBHs extracted from the list of Ho (2002), which will be the subject of a follow-up paper. As reported in Ho (2002) and Ho et al. (2003), NGC 821 has not been detected in radio continuum or optical emission lines (Hα and Hβ) and is a good example of a quiescent SMBH. Here we report the results of the *Chandra* ACIS observations of NGC 821 that have led to the discovery of an S-shaped feature suggestive of either a weak two-sided X-ray nuclear jet or hot shocked gas.

2. OBSERVATIONS AND DATA ANALYSIS

NGC 821 was observed with *Chandra* (Weisskopf et al. 2000) ACIS-S (principal investigator: Fabbiano) on 2002

[1] Harvard-Smithsonian Center for Astrophysics, 60 Garden Street, Cambridge, MA 02138; gfabbiano@cfa.harvard.edu; abaldi@cfa.harvard.edu; aneta@cfa.harvard.edu; elvis@cfa.harvard.edu; azezas@cfa.harvard.edu; jcm@cfa.harvard.edu.

[2] Dipartimento di Astronomia, Università di Bologna, via Ranzani 1, 40127 Bologna, Italy; silvia.pellegrini@unibo.it.

TABLE 1
NGC 821: Properties and *Chandra* ACIS-S Observation Log

$M^0_{B_T}$ (mag)	D (Mpc)	Diameter (arcmin) σ_0 (km s^{-1})	N_H (cm^{-2})	L_X, $L_{H\alpha}$ (ergs s^{-1})	M_{SMBH} (10^7 $M_\odot$)	0.″5 (pc)	ObsID	Date	T_{exp} (ks)
−20.71	23	2.6	6.2×10^{20}	$<5 \times 10^{40}$[a]	2.8–5.8[b]	55	4408	2002 Nov 26	24.6
...	...	209[c]	...	$<1.3 \times 10^{38}$[d]	...	...	4006	2002 Dec 1	13.3

Note.—Unless otherwise noted, the galaxy properties are as listed in NED.
[a] Beuing et al. (1999).
[b] Gebhardt et al. (2003), rescaled for the distance adopted here.
[c] Prugniel & Simien (1996).
[d] Ho et al. (2003).

November 26 (Observation ID 4408) and 2002 December 1 (ObsID 4006) for a total exposure time of 38 ks. Table 1 is a summary of the relevant properties of NGC 821 and the observing log.

No significant background flares were observed in these data, so no further screening was necessary. A time-dependent gain correction (Vikhlinin et al. 2003) was applied to the Standard Data Processing Level 2 event files before further analysis. The data were then analyzed using the CIAO version 3.0.1 software (CALDB 2.23) and XSPEC version 11.2.0 for the spectral fits.

2.1. *X-Ray Image*

The two observations were merged, taking into account the relative aspect solution of the two data sets, with the CIAO task *merge_all*. From the resulting data set, images were extracted in three spectral bands (red = 0.5–1 keV, green = 1–2 keV, and blue = 2–4 keV) covering the spectral range in which most source counts are detected. The images were then smoothed using *csmooth* with scales ranging from 1 to 20 pixels (0.″5–10″). Figure 1 shows the resulting "true-color" X-ray image of a 3′ field centered on NGC 821. Given the small region considered, no exposure correction was needed. The ellipse indicates the D_{25} isophote from RC3. Most of the X-ray emission is concentrated in the central regions of the galaxy, and it includes a diffuse component, a few pointlike sources, and a brighter central/nuclear region.

A higher resolution true-color image of the central region of NGC 821 is shown in Figure 2 (*left panel*), where the data are displayed at the original observed resolution without smoothing. This figure clearly shows a north-south elongated, hard central feature. Within the *Chandra* aspect uncertainties

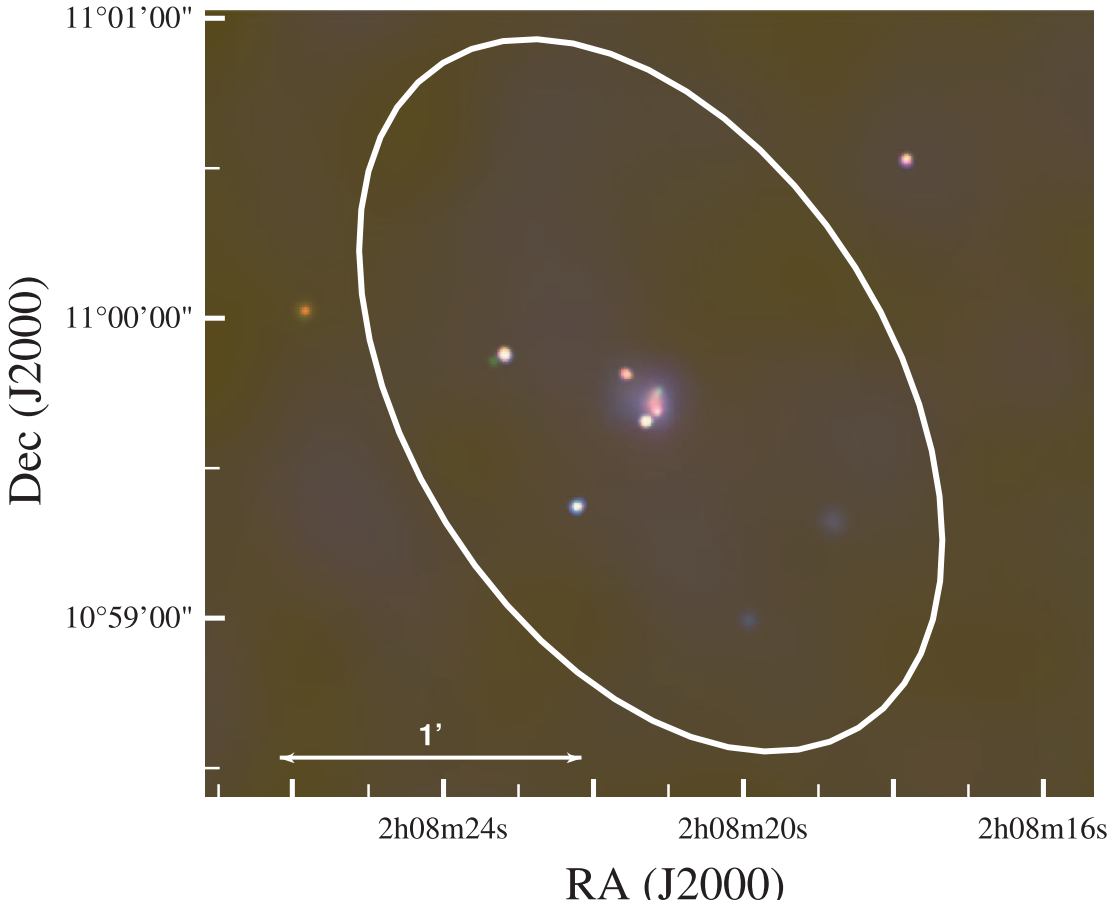

Fig. 1.—True-color adaptively smoothed image of NGC 821. The ellipse marks the 25th mag isophote.

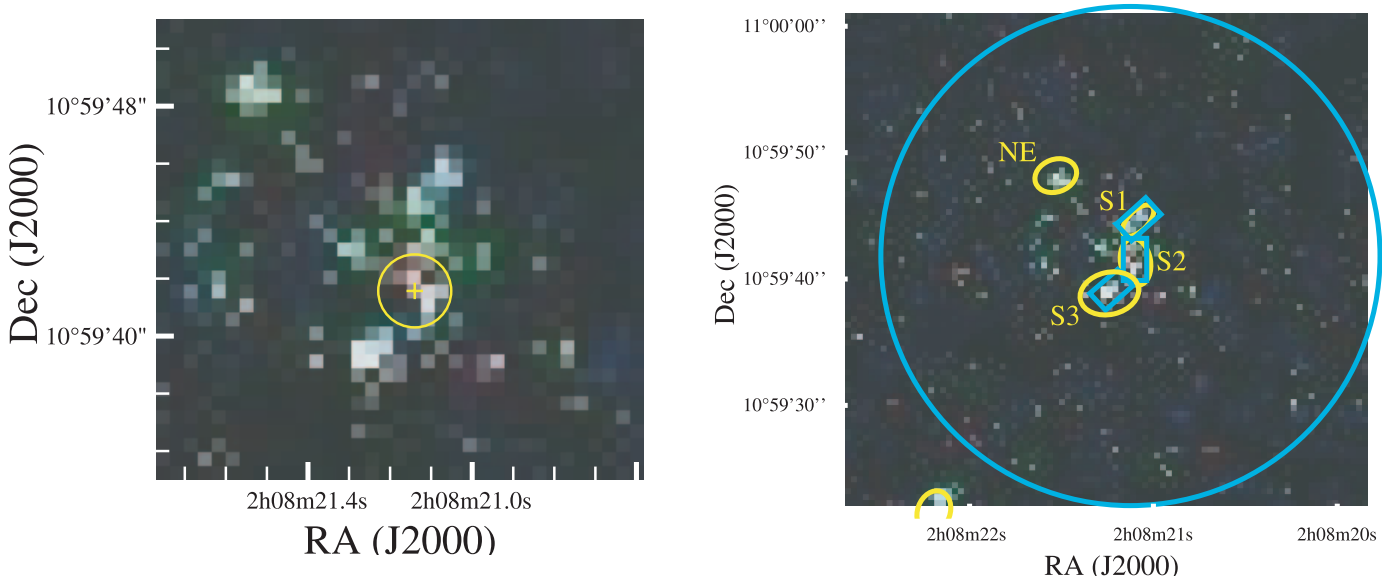

FIG. 2.—*Left panel:* True-color image of the central region of NGC 821, unsmoothed. The plus sign and surrounding circle represent the 2MASS nuclear position and uncertainty from NED. *Right panel:* Larger field image showing both the *wavdetect* source regions (*yellow*) and the spectral extraction regions for the "jet" and the diffuse emission (*light blue*).

(<0.″5), this feature is centered on the nucleus of NGC 821, at R.A. = $02^{h}08^{m}21^{s}.14$, decl. = +10°59′41.″7 (J2000, with uncertainty of 1.″25; from the Two Micron All Sky Survey [2MASS], as reported in the NASA/IPAC Extragalactic Database [NED]). While a pointlike source may be superposed on the southern tip of this elongated feature, the general form is suggestive of a two-sided bent jet, or S-shaped filament, centered on the nucleus. This feature is approximately 8.″5 long, corresponding to ~1 kpc at the distance of NGC 821.

2.2. *Point-Source Detection and Spatial Analysis of the Nuclear Feature*

We ran the CIAO *wavdetect* tool on the full-band ACIS image with scales between 2 and 4 pixels (1″–2″) and detected 11 sources (above 3 σ) in the area shown in Figure 1. We assume a power-law spectrum with $\Gamma = 1.8$ and Galactic $N_{\rm H} = 6.4\times10^{20}$ cm^{-2} (Stark et al. 1992), consistent with the emission of low-mass X-ray binaries (LMXBs) detected in early-type galaxies (see Kim & Fabbiano 2003). With this spectrum, the detected sources have 0.3–10 keV "emitted" fluxes in the 1.4×10^{-15}–1.4×10^{-14} ergs cm^{-2} s^{-1} range, corresponding to luminosities of 1.2×10^{38}–1.2×10^{39} ergs s^{-1}, if they indeed belong to NGC 821. The faintest sources we can detect in our exposure of NGC 821 are at the upper end of the luminosity distribution of the populations of LMXBs detected in other elliptical galaxies with *Chandra* (see, e.g., Kim & Fabbiano 2004). On the basis of these results, we expect that most LMXBs in NGC 821 will have $L_{\rm X} \leq 1\times10^{38}$ ergs s^{-1} and therefore will be undetectable. These LMXBs, however, will contribute to the unresolved "diffuse" galactic emission.

In the central region shown in Figure 2 (*left panel*), there are four sources: the isolated pointlike source at the northeast of the central complex (source NE, with 0.3–10 keV $L_{\rm X} = 4.7\times10^{38}$ ergs s^{-1}) and three sources in the central elongated emission region (identified by ellipses in the right panel of Fig. 2 and named S1, S2, and S3, from north to south). Further analysis (see below) demonstrates that these three central emission regions are not pointlike and therefore cannot be explained with the serendipitous positioning of three luminous galactic LMXBs in NGC 821. No discernible features can be seen in the optical image of NGC 821 at the positions of these three sources. Using the Deep Survey source counts in the 0.5–2 keV band (Rosati et al. 2002), the number of expected sources at fluxes of $\geq1.4\times10^{-15}$ ergs cm^{-2} s^{-1} is $\leq8\times10^{-3}$, so the chance detection of background sources is very unlikely. We cannot exclude a peculiar clustering of very luminous galactic X-ray binaries, and deeper data will be needed to explore this point further.

To establish the spatial properties of sources S1, S2, and S3, we have compared the spatial distribution of counts from each of them with that of the on-axis image of the quasar GB 1508+5714 (Siemiginowska et al. 2003a). GB 1508+5714 can be used as a good representation of the *Chandra* ACIS-S point-spread function (PSF) for our analysis, since the sources we are interested in are also at the aim point and similarly hard. With a count rate of ~0.05 count s^{-1}, the image of GB 1508+5714 (ObsID 2241) is not affected by pileup and contains 5300 counts within 2″ of the centroid of the count distribution. From this image, we determine the ratio of counts within the 1″–2″ annulus to those in the central 1″ radius circle to be *ratio* (PSF) = 0.043 ± 0.001 (1 σ). The isolated source NE in this central field yields *ratio* (NE) = 0.057 ± 0.054 (from a total of 36 source counts), entirely consistent with that of our reference quasar, confirming that GB 1508+5714 gives a good representation of the PSF. Instead, the analogous ratios for the background-subtracted counts from S1, S2, and S3 demonstrate that the emission is extended in all cases. Using the *wavdetect* centroids, we obtain *ratio* (S1) = 0.81 ± 0.26, *ratio* (S2) = 0.94 ± 0.27, and *ratio* (S3) = 0.29 ± 0.10. The total number of source counts in each of the three cases is 56, 67, and 71, respectively, larger than that for source NE. This comparison demonstrates that the spatial distributions of the source counts from S1 and S2 are definitely not consistent with the PSF. Although the spatial count distribution of S3 is more peaked and could contain a pointlike component, diffuse emission is also present. This analysis reinforces our suggestion that the central emission feature is intrinsically elongated.

Given that the central emission (S2) is not consistent with a point source, we can only estimate a 3 σ upper limit on the luminosity of a nuclear pointlike AGN. We used a 1″ × 1″ (2 × 2 pixel) sliding cell over the entire area covered by the

S-shaped feature and assumed as the background level the maximum value detected in the sliding cell. This conservative approach yields a 0.3–10 keV $L_X < 4.2 \times 10^{38}$ ergs s^{-1} for a power-law spectrum with $\Gamma = 1.8$ and line-of-sight Galactic N_H. This limit indicates that a central pointlike AGN would have a luminosity not exceeding that of normal LMXBs.

2.3. *Spectral Analysis*

We extracted spectral counts from both the S-shaped feature (regions in the right panel of Fig. 2) and the surrounding diffuse emission. The latter was taken from a 20″ circular region centered on the nucleus, excluding the S-shaped feature and the NE source. The field background was extracted from a source-free 50″ radius circular area 1.′8 from the nucleus of NGC 821. Spectral counts were extracted separately for the two observations using the CIAO script *acisspec*, which extracts a spectrum for both the source and the background region and creates weighted response matrices and ancillary response files (ARFs). The ARFs were corrected for the time-dependent degradation in the ACIS quantum efficiency using the CIAO script *apply_acisabs*. The source spectra from the two observations were then co-added (using the FTOOL *mathpha*) to optimize the signal-to-noise ratio of the data. We used the FTOOLS *addarf* and *addrmf* to combine the responses with their appropriate weights.

Hardness ratios (HR1 = $M-S/M+S$ and HR2 = $H-M/H+M$, where S = 0.5–1 keV, M = 1–2 keV, and H = 2–4 keV) are plotted (with 1 σ statistical errors) in Figure 3 and compared with power-law and Raymond-Smith emission models. The hardness ratios of the S1, S2, and S3 regions are all consistent with hard emission, either a power-law spectrum with Γ between $\sim$1 and $\sim$2.2 or thermal emission with $kT \sim 2$–20 keV. The diffuse X-ray emission of an elliptical galaxy is the combination of the soft emission of the hot ISM and the hard emission of the population of LMXBs below our detection threshold (see, e.g., Kim & Fabbiano 2003). In NGC 821 the hardness ratios of the diffuse emission are hard, suggesting a dominant LMXB component and little hot ISM.

With XSPEC, we fitted the data in the 0.3–10 keV energy range, rebinned to have at least 15 counts in each energy bin. For the S-shaped feature we adopted an absorbed power-law model [XSPEC model *wabs(wabs(pow))*], with N_H consisting of both a Galactic and an intrinsic component. The results of the fits are listed in Table 2, with 90% errors on one significant parameter. The S-shaped emission is well fitted with a power-law spectrum with $\Gamma \sim 1.8$, typical of AGN spectra, although the uncertainties are large. As discussed in § 2.2, there could be a possibly unrelated pointlike source at the southern tip of the S-shaped feature. Given the very few counts detected in our observations, we were unable to perform a meaningful spectral analysis, eliminating this source. However, the X-ray hardness ratios of Figure 3 show that the X-ray colors for the S1, S2, and S3 regions are remarkably similar and consistent with the power-law model derived from the minimum χ^2 fit.

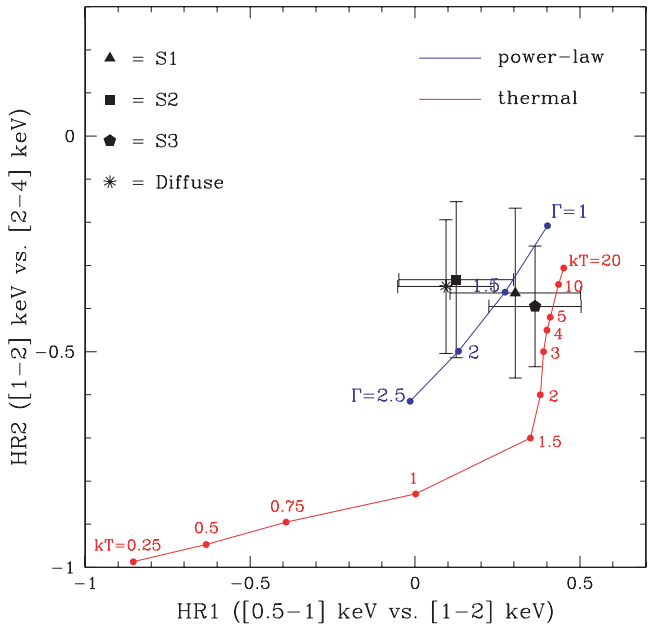

FIG. 3.—X-ray color-color diagram of "jet" and diffuse emission regions. Typical hardness ratios for a power-law model (Γ = 1–2.5) are plotted in blue. Typical hardness ratios for a thermal model (kT = 0.25–20 keV) are plotted in red. Galactic line-of-sight absorption ($N_H = 6.4 \times 10^{20}$ cm^{-2}; Stark et al. 1992) is assumed in both models.

For the diffuse emission, following, e.g., Kim & Fabbiano (2003), an optically thin thermal component was added to the power-law model [XSPEC model *wabs(wabs(apec+pow))*]. The metal abundance of the thermal component was fixed to 0.3 times the solar value (keeping the elemental solar ratios of Anders & Grevesse 1989). The spectrum of the diffuse galactic emission (see Table 2) is consistent with a hot gas with a temperature $kT \sim 0.5$ keV or cooler, typical of X-ray–faint early-type galaxy halos (e.g., Pellegrini & Fabbiano 1994; Irwin & Sarazin 1998). The power-law component, although ill-defined, is needed to obtain an acceptable fit for the diffuse emission, as clearly suggested by Figure 3; this is in agreement with the presence of an unresolved LMXB population. The χ^2 for a simple thermal model (*APEC*; Smith et al. 2001) is 25.8 with 12 degrees of freedom (dof). Comparing this with the two-component χ^2 by means of an F-test, we obtain a chance probability of 10^{-3}. Fitting the diffuse emission with a single power-law model also results in a worse χ^2, but in this case the F-test probability is only 12%. While the two-component model is plausible for the diffuse emission, the rather low signal-to-noise ratio of our data does not allow a stronger discrimination among models. In the following discussion we will use the results of the two-component model

TABLE 2
RESULTS OF SPECTRAL FITS

Component	Net Counts (0.3–10 keV)	χ^2/dof	N_H ($\times 10^{21}$ cm^{-2})	kT (keV)	Γ	L_X(0.3–10 keV) (ergs s^{-1})
S-shaped	141	6.7/5	$1.41^{+1.84}_{-1.41}$	...	$1.82^{+0.71}_{-0.56}$	$2.6 \pm 0.5 \times 10^{39}$
	...	6.5/5	$0.75^{+2.34}_{-0.75}$	$5.14^{+50.00}_{-2.99}$	...	$1.9^{+1.4}_{-0.4} \times 10^{39}$
Diffuse.....	174	6.5/10	<9.00	$0.46^{+0.33}_{-0.25}$	$1.27^{+1.13}_{-0.68}$	$3.5 \pm 0.6 \times 10^{39}$
Thermal	...	...	...	...	...	$3.4 \pm 0.1 \times 10^{38}$

fit; however, deeper observations of NGC 821 are essential to firmly constrain the characteristics of the hot ISM in this galaxy.

Table 2 also lists the best-fit unabsorbed luminosities for the S-shaped feature, the total diffuse emission, and the thermal component of the diffuse emission. The latter is only 10% of the total diffuse emission, indicating that NGC 821 is singularly devoid of hot ISM. Strictly speaking, we have a 90% upper limit of 3.5×10^{38} ergs s^{-1} on the luminosity of the gaseous component. The uncertainties of these luminosities reflect the uncertainties of the spectral parameters. From the emission measure of the soft thermal component we estimate an "indicative" electron density $n = 4.1^{+10.9}_{-1.5}\times10^{-3}$ cm^{-3}. While deeper data are needed for a definite measure, the above estimate is useful for gaining first-cut insights into the nature of the S-shaped feature, and in this spirit we use it in the following discussion.

3. DISCUSSION

NGC 821 was observed with *Chandra* because the existing *ROSAT* upper limit on the X-ray luminosity of its nuclear SMBH implied extremely sub-Eddington nuclear emission. Our observations fail to detect a pointlike source at the nucleus, down to a 3 σ limit of $L_X(0.3\text{–}10\ \mathrm{keV}) < 4.2\times10^{38}$ ergs s^{-1}, $\sim$100 times fainter than the *ROSAT* limit (see Table 1). The nucleus is not detected in the far-infrared or in H_2 (Georgakakis et al. 2001), arguing against a strongly obscured AGN (and against a nuclear starburst). There is also no sign of a strong intrinsic absorbing column in the X-rays (see Table 2). The general AGN "quiescent state" is also supported by the lack of radio continuum and optical line emission (Ho 2002; Ho et al. 2003). We detect instead an elongated, possibly bent, emission feature, strongly suggestive of a two-sided X-ray jet or S-shaped filament. This feature, extending over $\sim$1 kpc, has a hard spectrum consistent with a power law with best-fit $\Gamma \sim 1.8^{+0.7}_{-0.6}$ ($\alpha = 0.8$) or, if thermal, $kT > 2$ keV. The X-ray luminosity of this feature is $\sim1.9\text{–}2.6\times10^{39}$ ergs s^{-1}, corresponding to $\sim5\times10^{-7}$ of the Eddington luminosity of the SMBH.

The nature of this intriguing elongated feature is investigated below. We consider the possibilities of a two-sided jet (§ 3.1), thermal emission from gas heated by some form of energy deposition resulting from nuclear activity (§§ 3.2 and 3.3), and unresolved LMXB emission (§ 3.4).

3.1. *Is a Jet Directly Emitting the Hard X-Rays?*

Here we discuss the possibility that the S-shaped hard emission centered on the nucleus of NGC 821 is a two-sided nuclear jet, as in radio galaxies. The spectral power-law slope of this emission has large uncertainties (Table 2) but is consistent with the X-ray spectra of other jets (Siemiginowska et al. 2003b; Sambruna et al. 2004). However, unlike other extragalactic X-ray jets seen in luminous AGNs, where $L_X(\mathrm{jet})/L_X(\mathrm{AGN}) \sim 1\%\text{–}15\%$ (e.g., Schwartz et al. 2003), this "jet" has no associated core X-ray source, implying $L_X(\mathrm{jet})/L_X(\mathrm{AGN}) > 6$. This lack of core emission also differs from other X-ray–weak AGNs in which only a point X-ray source has been seen, typically in nuclei with radio detections, and these are usually modeled as Comptonized jets (Baganoff et al. 2001; Markoff et al. 2001; Fabbiano et al. 2003). An exception is M87, with its core-jet structure (Di Matteo et al. 2001). The NGC 821 "jet" could be similar to the somewhat steeper spectrum ($\Gamma \sim 2.3$) of the M87 jet (Wilson & Yang 2002), in which the nuclear pointlike AGN is fainter compared with the jet [$L_X(\mathrm{jet})/L_X(\mathrm{AGN}) \sim 2$]. The 0.5 kpc (one-sided) scale of the NGC 821 "jet" is also similar to the $\sim$1.5 kpc of the M87 jet, while most radio/X-ray jets extend over much larger distances, up to 300 kpc (Siemiginowska et al. 2002, 2003b). The NGC 821 "jet" is two-sided, putting a limit on relativistic beaming and suggesting only a relatively slow expansion ($v < 0.3c$; see, e.g., Leahy 1991). The typical expansion velocity of the M87 jet is $0.5c$, although small features can reach 4–6c (Biretta et al. 1995, 1999).

If a jet is present, we can make some simple estimates of the activity timescale and the energetics involved. First, based on the above limit on the expansion velocity ($v < 0.3c$), we can relate the size of the jet to the activity timescale, finding that the jet may have been propagating for a few thousand years, assuming free unimpeded propagation. However, it is more likely that the jet is disrupted by interaction with the surrounding hot ISM ($n = 4.1^{+10.9}_{-1.5}\times10^{-3}$ cm^{-3}) as, for example, may be occurring in NGC 1316, which has a similar ISM density (0.01 cm^{-3} in the jet disruption region; Kim et al. 1998). Theoretical simulations (De Young 1993) of jet propagation into a homogeneous ISM indicate that hot ISM with densities of 0.01 particles cm^{-3}, similar to that of NGC 821, can significantly slow down a jet 10^5 times more powerful than the one we may have in NGC 821.

Considering that the jet is likely to interact with the surrounding hot ISM, its size may be indicative of equilibrium between the ram pressure of the expanding jet and the thermal pressure of the hot ISM. We estimate the thermal pressure of the ISM from the diffuse X-ray emission to be $\sim1.5\times10^{-11}$ dyne cm^{-2} ($P_{\mathrm{th}} = 2n_e kT$). Equating this pressure to the ram pressure $P_{\mathrm{ram}} = \rho_{\mathrm{ISM}} v^2$, where ρ_{ISM} is the mass density of the ISM, we derive a jet expansion velocity v of $0.043c$. This estimate is a lower limit, since the density in the jet is unknown and it is likely to be smaller than ρ_{ISM}. This estimate of V is consistent with the upper limit mentioned earlier and corresponding to a jet expansion (or activity) timescale of 3.8×10^4 yr. The jet kinetic energy can be estimated from $E_{\mathrm{kin}} = 0.5P_{\mathrm{ram}}V$, where V is the volume occupied by the jet. To calculate V, we assumed a jet thickness of 10 pc and length of 1 kpc, obtaining $V = 2.7\times10^{60}$ cm^3. The kinetic energy input to this volume is then 4.1×10^{49} ergs, and by dividing this E_{kin} by the jet expansion time we derive a kinetic luminosity of 1.7×10^{37} ergs s^{-1}. This is $\sim$100 times smaller than the X-ray luminosity. However, this may be a lower limit if the jet is "overpressured," as in M87, where the radio cavities in the cluster gas suggest overpressurization by a factor of $\sim$3 with respect to the cluster gas (Reynolds 1997; Reynolds et al. 1996). However, M87 has a jet kinetic luminosity of $\sim10^{43}$ ergs s^{-1} and a radiative power of $\sim10^{42}$ ergs s^{-1}, far more powerful than the jet in NGC 821.

What would be the emission mechanism responsible for the S-shaped emission of NGC 821 in the jet hypothesis? Synchrotron emission is plausible: $\alpha_{\mathrm{radio-X}} \leq 0.7$ (estimated from the radio flux limit of 0.5 mJy at 5 GHz and the X-ray flux at 1 keV) is consistent with the X-ray slope and typical of the synchrotron slope observed in radio lobes (Peterson 1997). The usual problem of short synchrotron lifetime for X-ray–producing electrons (Feigelson et al. 1981) implies local particle reacceleration 0.5 kpc from the nucleus. A radio detection not far below the current limit is expected if synchrotron radiation produces the S-shaped emission at the center of NGC 821. The NGC 821 emission could be consistent with the M87 jet also in this respect: Wilson & Yang (2002) find $\alpha_{\mathrm{radio-X}} \sim 0.9$ for the knots of the M87 jet, and they prefer a synchrotron origin for the X-ray emission of these knots. A value of $\alpha_{\mathrm{radio-X}} \leq 0.7$ is also consistent with the values of $\alpha_{\mathrm{radio-X}} = 0.7\text{–}0.8$ reported for knots in powerful jets by Sambruna et al. (2004), who favor an inverse Compton origin for the X-ray flux.

However, in our case we find that this mechanism cannot explain the emission for plausible sources of seed photons, including synchrotron photons within the jet (the "self-Compton" case) and the optical photon field from the intense starlight in the center of NGC 821.

3.2. *Is Hot Gas Responsible for the Hard Emission?*

Here we examine the possibility that the origin of the hard S-shaped emission is thermal. We consider two scenarios suggested by analogies with other galaxies: thermal emission from the jet-ISM interaction, as in NGC 1052 (Kadler et al. 2004), and shocks in the ISM resulting from an outburst of nuclear activity, as suggested in the case of NGC 4636 (Jones et al. 2002).

An elongated feature in the central galaxy region, of temperature $kT \sim 0.5$ keV, was found with *Chandra* in NGC 1052, the prototype elliptical galaxy LINER (also at a distance of 22.6 Mpc; Knapp et al. 1978). This feature has 10 times the flux of the S-shaped emission in NGC 821 ($\sim 3.5 \times 10^{-13}$ ergs cm^{-2} s^{-1}) and about double the linear size (Kadler et al. 2004). In NGC 1052 the extended emission has radio and optical counterparts and may be more fan-shaped than linear, although the photon statistics are limited in this short (2.3 ks) ACIS observation. Kadler et al. suggest shock heating of gas, converting some of the kinetic energy of the observed radio jet into X-ray emission. In the case of NGC 821, if a jet is present, it could similarly deposit energy in the surrounding ISM, causing it to produce the hard thermal emission. However, if its kinetic power is on the order of that estimated in § 3.1 ($\sim 10^{37}$ ergs s^{-1}), this mechanism cannot explain the luminosity of the hard thermal emission measured with ACIS ($L_{\rm X} \sim 1.9 \times 10^{39}$ ergs s^{-1}; Table 2). Unless a jet is present with kinetic power that is orders of magnitude larger, other sources of energy deposition are needed.

An alternative analogy is offered by the hot "arms" of NGC 4636 (Jones et al. 2002), a giant elliptical galaxy in Virgo with no reported nuclear activity or jets. These arms, with a larger spatial scale (8 kpc) and a lower temperature ($\sim$0.5–0.7 keV) than the S-shaped feature of NGC 821, are two symmetric features crossing the galaxy center that were discovered in the *Chandra* ACIS data of NGC 4636. The NGC 4636 arms are accompanied by a temperature increase with respect to the surrounding hot ISM, which led to the suggestion by Jones et al. of shock heating of the ISM caused by a nuclear outburst. We discuss this process at the end of § 3.3, in the unsteady accretion hypothesis. As discussed in § 2.3, the S-shaped feature of NGC 821 could similarly be hotter than its surroundings. Assuming a temperature of $kT = 3$ keV for this feature, close to the lower limit suggested by our spectral fit (Table 2), we obtain a density $n = 8.59^{+1.06}_{-1.07}$ cm^{-3} (errors at 90%). Using the best-fit value (and a temperature of 3 keV), we obtain a thermal pressure exceeding by a factor of $\sim$14 that quoted in § 3.1 for the surrounding hot ISM, suggesting a nonequilibrium situation, if only thermal pressures are involved. However, given the uncertainties in both T and n, the thermal pressures of both the S-shaped feature and the surrounding ISM could be similar. It is clear that deeper *Chandra* observations are needed to better constrain the energetics of this feature.

3.3. *Is Accretion Present?*

Whether it is a jet or hot shocked gas, the S-shaped feature of NGC 821 requires a considerable energy input, an obvious source of which is accretion onto the nuclear SMBH. Taking at face value the indication of the two-component fit of the circumnuclear diffuse emission, which is consistent with the presence of a $kT \sim 0.5$ keV thermal component, we can estimate the nuclear accretion rate using the steady spherical accretion scenario of Bondi (1952). This estimate is rough because the gravitational capture radius (which depends on the gas temperature and the mass of the SMBH; see the textbook by Frank et al. 2002) is, in our case, $r_{\rm acc} \sim 3$–23 pc, smaller than the physical resolution of the image (55 pc; Table 1). In this estimate of $r_{\rm acc}$ we have allowed for the uncertainties in both the SMBH mass and kT. Based on the circumnuclear gas temperature and density, which we estimate from the emission measure of the diffuse thermal component to be $n = 4.1^{+10.9}_{-1.5} \times 10^{-3}$ cm^{-3}, the Bondi mass accretion rate (also following Frank et al. 2002) is $\dot{M}_{\rm acc} = 1.1 \times 10^{-7}$–$2.0 \times 10^{-5}\ M_{\odot}\ {\rm yr}^{-1}$, including again all the uncertainties in the SMBH mass, kT, and n. The corresponding luminosity is $L_{\rm acc} = 6.2 \times 10^{38}$–$1.1 \times 10^{41}$ ergs s^{-1}, with the customary assumption of 10% accretion efficiency. The luminosity of the S-shaped feature is within this range; therefore, in principle it could be explained by Bondi accretion of the hot ISM. This conclusion, however, is most certainly not correct, because comparison with independent optical data, discussed below, shows that our uncertain X-ray data may have led to underestimating the circumnuclear gas density and therefore $\dot{M}_{\rm acc}$.

Since the hot ISM is the thermalized integrated result of the stellar mass losses, at a minimum one expects the total stellar mass loss rate $\dot{M}_*$ within $r_{\rm acc}$ to be accreted (there may also be gas inflowing from outside $r_{\rm acc}$). The value of $\dot{M}_*$ can easily be obtained from the luminosity density profile recovered from *HST* data for the central galaxy region (Gebhardt et al. 2003). Using a conversion factor from luminosity to mass loss rate for an old stellar population at the present epoch (e.g., Ciotti et al. 1991), this leads to $\dot{M}_* = 9.8 \times 10^{-6}$ and $2.6 \times 10^{-4}\ M_{\odot}\ {\rm yr}^{-1}$ for the two extreme values of $r_{\rm acc}$. These $\dot{M}_*$ values are, respectively, a factor of $\sim$90 and $\sim$13 larger than the $\dot{M}_{\rm acc}$ values derived above for the same $r_{\rm acc}$. Given that this estimate of $\dot{M}_*$ is quite robust, we must conclude that either the derivation of $\dot{M}_{\rm acc}$ above is inaccurate, or the gas is not steadily inflowing within $r_{\rm acc}$. The former possibility cannot be excluded with the present data, since in our calculation of $\dot{M}_{\rm acc}$ we used a density n-value that is an average measured over a region extending much farther out than $r_{\rm acc}$; $n(r_{\rm acc})$ is likely to be significantly higher than this average (e.g., a factor of $\sim$30 times higher, for an $n \propto r^{-0.9}$ profile).

Assuming that it is just the stellar mass loss rate within $r_{\rm acc}$ that is steadily accreted, accretion luminosities greater than 20 times larger than the observed $L_{\rm X}$ of the hard emission are recovered (from $L_{\rm acc} = 0.1 \dot{M}_* c^2$). Then the "solutions" proposed for the other X-ray–faint nearby nuclei must be revisited for NGC 821. These are (1) accretion occurs but with low radiative efficiency (e.g., Narayan 2002); (2) accretion sustains a jet (this can be coupled again with a low radiative efficiency) whose total power is of the order of $L_{\rm acc}$, as in the modeling for IC 1459 (Fabbiano et al. 2003) and M87 (Di Matteo et al. 2003); and (3) accretion is unsteady and therefore the hot ISM in the nuclear region need not be inflowing (Siemiginowska et al. 1996; Janiuk et al. 2004). In this case the feedback from the central SMBH can be either radiative (Ciotti & Ostriker 2001) or mechanical (Binney & Tabor 1995; Omma et al. 2004) and make accretion undergo activity cycles. While active, the central engine heats the surrounding ISM, so that radiative cooling—and accretion—are offset; then the central engine turns off until the ISM starts cooling again and accretion resumes.

NGC 821 may be in a stage of such a cycle when a nuclear outburst has recently occurred. Note that the accretion luminosity that is radiatively absorbed by the ISM during an outburst (Ciotti & Ostriker 2001) largely exceeds the hard thermal emission observed at the center of NGC 821.

If the S-shaped feature is of nonstellar origin (see below), its being hotter than the surrounding gas would be evidence that central heating is at work, and therefore some type of feedback from the SMBH is occurring. The unsteady scenario seems promising as an adequate fit for the case of NGC 821; this galaxy is clearly hot-gas–poor, as if recently swept by an outburst-driven wind. From our ACIS-S data we estimate an upper limit of $\sim 4 \times 10^6\ M_\odot$ on the amount of hot ISM, many orders of magnitude smaller than that for hot-gas–rich ellipticals (see Fabbiano 1989).

3.4. *LMXB Emission?*

In § 2 we considered the possibility that the S-shaped emission may result from an asymmetric distribution of LMXBs in the central region of NGC 821. Its spectral properties, as discussed there, are certainly consistent with hard LMXB emission. While we can dismiss the possibility that three luminous LMXBs are responsible for the emission, based on the spatial extent of the three detected sources in this region, we cannot exclude an elongated spatial distribution of a larger number of fainter sources. While LMXBs in early-type galaxies are usually distributed to follow the stellar light (e.g., Kim & Fabbiano 2003), departures from this behavior have been detected (e.g., Zezas et al. 2003). In the bulge of M31, there is a barlike central distribution of sources of approximately 1 kpc extent (Van Speybroeck et al. 1979; Trinchieri & Fabbiano 1991). Deeper observations are needed to investigate the possibility that the S-shaped feature is the tip of the iceberg of the LMXB population.

4. CONCLUSIONS

We have shown that NGC 821, which is used as template of a quiescent and normal "old elliptical" (see, e.g., Ho et al. 2003), may show signs of energy deposition by the nucleus: an elongated, bent, kiloparsec-sized, S-shaped feature centered (within the $\sim 1\farcs5$ errors) on the nucleus. This feature has $L_X \sim 1.9$–2.6×10^{39} ergs s^{-1} (0.3–10 keV) and a hard spectrum consistent with a power law with $\Gamma \sim 1.8$ or thermal emission with $kT > 2$ keV. It may be embedded in a faint hot ISM with $kT \sim 0.5$ keV.

This feature could represent the faintest extragalactic jet yet reported. We can exclude inverse Compton (of either radio photons or the central stellar photon field) as an explanation of the X-ray emission. If this feature is indeed a nonthermal jet, this leaves synchrotron as a possible explanation. The $\alpha_{\rm radio-X} \leq 0.7$ would be consistent with this hypothesis. In the jet scenario, we constrain the activity timescale to be $\sim 4 \times 10^4$ yr. We also estimate that most of the power in this jet may be in X-ray radiation, rather than kinetic energy.

Alternatively, the emission could be thermal. It is unlikely that the detected luminosity could result from interaction of a jet with the surrounding ISM in this galaxy (as may occur, e.g., in NGC 1052; Kadler et al. 2004) because the jet kinetic power would be orders of magnitude below the detected X-ray luminosity. A more likely scenario is that of S-shaped shocks of the hot ISM, driven by an outburst of nuclear activity, as suggested in the case of NGC 4636 (Jones et al. 2002). Accretion from stellar mass loss rate in the circumnuclear region would produce a luminosity well in excess of the detected one, suggesting either low radiative efficiency (e.g., Narayan 2002) or unsteady accretion (e.g., Binney & Tabor 1995; Siemiginowska et al. 1996; Ciotti & Ostriker 2001). The second scenario is supported by the very small amount of hot ISM of NGC 821. Whether and how an S-shaped structure can be created remains unexplored by the current modeling of outbursts through hydrodynamical simulations.

It is only in the X-ray band, thanks to the *Chandra* spatial resolution, that possible signs of nuclear activity are found in NGC 821. Either the jet or the shock explanation of the S-shaped nuclear feature detected with *Chandra* suggests a fairly recent nuclear outburst, now spent. However, the present data are not deep enough to allow either a detailed study of the morphology and spectral parameters of this feature or a model-independent detection of the circumnuclear hot ISM. More important, while the present data are not consistent with three pointlike sources originating in the three detected emission regions, a population of fainter LMXBs in a barlike distribution cannot be excluded. A significantly deeper *Chandra* exposure is needed to answer the many questions raised by the present data. Deeper Very Large Array data are also needed to set a tighter constraint on the jet scenario.

We thank Roberto Soria for comments and the *Chandra* X-Ray Center DS and SDS teams for their efforts in reducing the data and developing the software used for the data reduction (SDP) and analysis (CIAO). We have used the NASA-funded services NED and ADS and browsed the *Hubble* archive. This work was supported by NASA contract NAS 8-39073 (CXC) and NASA grant GO3-4133X.

REFERENCES

Anders, F., & Grevesse, N. 1989, Geochim. Cosmochim. Acta, 53, 197
Baganoff, F. K., et al. 2001, Nature, 413, 45
Beuing, J., Döbereiner, S., Böhringer, H., & Bender, R. 1999, MNRAS, 302, 209
Binney, J., & Tabor, G. 1995, MNRAS, 276, 663
Biretta, J. A., Sparks, W. B., & Macchetto, F. 1999, ApJ, 520, 621
Biretta, J. A., Zhou, F., & Owen, F. N. 1995, ApJ, 447, 582
Bondi, H. 1952, MNRAS, 112, 195
Ciotti, L., & Ostriker, J. P. 2001, ApJ, 551, 131
Ciotti, L., Pellegrini, S., Renzini, A., & D'Ercole, A. 1991, ApJ, 376, 380
De Young, D. 1993, ApJ, 402, 95
de Zeeuw, P. T., et al. 2002, MNRAS, 329, 513
Di Matteo, T., Allen, S. W., Fabian, A. C., Wilson, A. S., & Young, A. J. 2003, ApJ, 582, 133
Di Matteo, T., Carilli, C. L., & Fabian, A. C. 2001, ApJ, 547, 731
Fabbiano, G. 1989, ARA&A, 27, 87
Fabbiano, G., & Juda, J. 1997, ApJ, 476, 666
Fabbiano, G., et al. 2003, ApJ, 588, 175
Feigelson, E. D., Schreier, E. J., Delvaille, J. P., Giacconi, R., Grindlay, J. E., & Lightman, A. P. 1981, ApJ, 251, 31
Ferrarese, L., & Merritt, D. 2000, ApJ, 539, L9
Frank, J., King, A., & Raine, D. J. 2002, Accretion Power in Astrophysics (3rd ed.; Cambridge: Cambridge Univ. Press)
Gebhardt, K., et al. 2000, ApJ, 539, L13
———. 2003, ApJ, 583, 92
Georgakakis, A., Hopkins, A. M., Caulton, A., Wiklind, T., Terlevich, A. I., & Forbes, D. A. 2001, MNRAS, 326, 1431
Graham, A. W., Erwin, P., Caon, N., & Trujillo, I. 2001, ApJ, 563, L11
Ho, L. C. 2002, ApJ, 564, 120
Ho, L. C., Filippenko, A. V., & Sargent, W. L. W. 2003, ApJ, 583, 159
Ho, L. C., et al. 2001, ApJ, 549, L51
Irwin, J. A., & Sarazin, C. L. 1998, ApJ, 499, 650
Janiuk, A., Czerny, B., Siemiginowska, A., & Szczerba, R. 2004, ApJ, 602, 595

Jones, C., Forman, W., Vikhlinin, A., Markevitch, M., David, L., Warmflash, A., Murray, S., & Nulsen, P. E. J. 2002, ApJ, 567, L115
Kadler, M., Kerp, J., Ros, E., Falcke, H., Pogge, R. W., & Zensus, J. A. 2004, A&A, 420, 467
Kim, D.-W., & Fabbiano, G. 2003, ApJ, 586, 826
———. 2004, ApJ, 611, 846
Kim, D.-W., Fabbiano, G., & Mackie, G. 1998, ApJ, 497, 699
Knapp, G. R., Faber, S. M., & Gallagher, J. S. 1978, AJ, 83, 139
Leahy, J. P. 1991, in Beams and Jets in Astrophysics, ed. P. A. Hughes (Cambridge: Cambridge Univ. Press), 100
Loewenstein, M., Mushotzky, R. F., Angelini, L., Arnaud, K. A., & Quataert, E. 2001, ApJ, 555, L21
Magorrian, J., et al. 1998, AJ, 115, 2285
Markoff, S., Falcke, H., Yuan, F., & Biermann, P. L. 2001, A&A, 379, L13
Martini, P., Pogge, R. W., Ravindranath, S., & An, J. H. 2001, ApJ, 562, 139
Narayan, R. 2002, in Lighthouses of the Universe: The Most Luminous Celestial Objects and Their Use for Cosmology, ed. M. Gilfanov, R. Sunyaev, & E. Churazov (Berlin: Springer), 405
Omma, H., Binney, J., Bryan, G., & Slyz, A. 2004, MNRAS, 348, 1105
Pellegrini, S., Baldi, A., Fabbiano, G., & Kim, D.-W. 2003a, ApJ, 597, 175
Pellegrini, S., & Fabbiano, G. 1994, ApJ, 429, 105
Pellegrini, S., Venturi, T., Comastri, A., Fabbiano, G., Fiore, F., Vignali, C., Morganti, R., & Trinchieri, G. 2003b, ApJ, 585, 677
Peterson, B. M. 1997, An Introduction to Active Galactic Nuclei (Cambridge: Cambridge Univ. Press)
Phinney, E. S. 1983, Ph.D. thesis, Univ. Cambridge
Prugniel, P., & Simien, F. 1996, A&A, 309, 749
Ravindranath, S., Ho, L. C., Peng, C. Y., Filippenko, A. V., & Sargent, W. L. W. 2001, AJ, 122, 653
Rees, M. J. 1984, ARA&A, 22, 471
Reynolds, C. S. 1997, Ph.D. thesis, Univ. Cambridge
Reynolds, C. S., Fabian, A. C., Celotti, A., & Rees, M. J. 1996, MNRAS, 283, 873
Richstone, D., et al. 1998, Nature, 395A, 14
Rosati, P., et al. 2002, ApJ, 566, 667
Sambruna, R. M., Gambill, J. K., Maraschi, L., Tavecchio, F., Cerutti, R., Cheung, C. C., Urry, C. M., & Chartas, G. 2004, ApJ, 608, 698
Schwartz, D. A., et al. 2003, NewA Rev., 47, 461
Siemiginowska, A., Bechtold, J., Aldcroft, T. L., Elvis, M., Harris, D. E., & Dobrzycki, A. 2002, ApJ, 570, 543
Siemiginowska, A., Czerny, B., & Kostyunin, V. 1996, ApJ, 458, 491
Siemiginowska, A., Smith, R. K., Aldcroft, T. L., Schwartz, D. A., Paerels, F., & Petric, A. O. 2003a, ApJ, 598, L15
Siemiginowska, A., et al. 2003b, ApJ, 595, 643
Smith, R. K., Brickhouse, N. S., Liedahl, D. A., & Raymond, J. C. 2001, ApJ, 556, L91
Stark, A. A., Gammie, C. F., Wilson, R. W., Bally, J., Linke, R. A., Heiles, C., & Hurwitz, M. 1992, ApJS, 79, 77
Trinchieri, G., & Fabbiano, G. 1991, ApJ, 382, 82
van der Marel, R. P. 1999, AJ, 117, 744
Van Speybroeck, L., Epstein, A., Forman, W., Giacconi, R., Jones, C., Liller, W., & Smarr, L. 1979, ApJ, 234, L45
Vikhlinin, A., Schulz, N., Tibbetts, K., & Edgar, R. 2003, Corrections for Time Dependence of ACIS Gain, http://cxc.harvard.edu/contrib/alexey/tgain/tgain.html
Weisskopf, M., Tananbaum, H., Van Speybroeck, L., & O'Dell, S. 2000, Proc. SPIE, 4012, 2
Wilson, A. S., & Yang, Y. 2002, ApJ, 568, 133
Zezas, A., Hernquist, L., Fabbiano, G., & Miller, J. 2003, ApJ, 599, L73